Experimental and Numerical Study on Effect of Fibre Orientations on Residual Elastic Properties in Glass Fibre Laminates.

Destayehu Addisu^{1*}, Ermias G/Kidan Koricho^{2*}, and Addisu Negash^{1*}, Getnet Ayele¹

¹Bahir Dar University, Bahir Dar Institute of Technology, Faculty of Mechanical and Industrial Engineering, Bahir Dar, Ethiopia.

²Addis Ababa Science and Technology University.

Abstract: - This work combines experimental and numerical studies on the free vibration of glass fiber-reinforced polymer (GFRP). The effect of fiber orientations of GFRP composite laminated materials has been investigated by vibration characteristics. Three symmetric laminates having [(0/90)3] S, [(30/-60)3] S and [(45/-45)3] S fiber orientation angles were prepared using plain weave glass fabrics as reinforcement. Residual elastic characteristics of GFRP composite laminated materials have been investigated concerning the effect of angle ply orientations. The vibration study is carried out using an accelerometer and numerical analysis was carried out using ABAQUS with different boundary conditions. It is observed from the results that GFRP with different fiber orientations yields different residual elastic properties by considering the same load, size & shape constraints. It is observed from the result that GFRP with [00/900]3 fiber orientation Yields high (residual elastic) strength when compared to other degrees of orientations for the same load, size & shape addition.

Keywords: Residual elastic properties, Degree of orientation, Vibration study; glass-polyester, and experimental and Numerical analysis.

1. Introduction

Nowadays, composite materials are the most used materials in the development of industries in various fields. It was commonly used in structural mechanical applications due to its lightweight, mechanical strength and stiffness, corrosion resistance, energy absorption capacity, and noise attenuation optimal characteristics. However, many factors limit their widespread applications, such as the high cost of raw materials or requirements for high production volumes. Among the others, the complexity of the damage evolution plays a key role in their application limitations, especially for structural component applications. Several interacting failure modes are typical of composite materials and a progressive and rapid decrement of the mechanical properties is a common challenge [1]. In this context, methods to assess damage levels and predict residual structural strength in composites are becoming increasingly important.

Vibration is a mechanical phenomenon whereby oscillations occur at an equilibrium point. Vibrations are undesirable for a mechanical structure, due to the need for structural stability, position control durability (particularly durability against fatigue), performance, and noise reduction. Vibrations are of concern to large structures such as aircraft, as well as small structures such as electronics. Nowadays, it has been used in electronics, aviation, automobile application, etc. Composite materials are having excellent mechanical, tribological, thermal, water absorption, and vibrational proper-ties. Moreover, the use of composites to fabricate structures is one of the ways to reduce vibrations.

Due to this usage, the high specific strength and stiffness of laminated composite materials are becoming more prevalent in many structural applications. Fiber-reinforced composite materials (FRCM) are chosen for weight-critical applications because they offer favourable ratings for fatigue failure. The objective of this work is to forecast each laminate's local residual elastic characteristics under vibration analysis for three different orientation

angles. This work establishes crucial test protocols for the FRCM to be employed in specific structural applications, with a primary focus on the impact of angle orientation on the residual elastic properties.

Polymer matrix composite (PMC) with fiber-shaped reinforcements is the form of composite that is utilized the most frequently. The most popular matrix material for creating PMCs is polyester resin. [1] A number of composites are used in a wide range of applications across numerous industries. The type of matrix and reinforcement, form and size, final product qualities, and intended purpose are the main determinants of the fabrication procedure. [2] Performing a wet layup procedure in an auto-clave or using a vacuum bagging technique is a typical method of producing composites. These techniques offer a composite that is almost void-free and give you more control over the thickness and fiber content of the moulded object. Composites ac-quire internal resistance to deformations in the form of stresses, much like metals and alloys do. Only when composite material is loaded in any way can these stresses occur. Composite materials, much like metals and alloys, are susceptible to the development of residual elastic characteristics, which exist even in the absence of loading. Based on responses to released residual elastic qualities, changes in failure patterns, modifications to the material's structure, and reactions to temperature changes, residual elastic properties can be determined.

In recent years, fiber-reinforced composite laminate materials have increased significantly in structural applications due to their improved and superior properties. The properties of fiber-reinforced composite materials depend on several parameters such as the material of fiber and matrix, curing process, fiber orientation, stacking sequence, inherent lamina, and laminate level flaws introduced during the manufacturing process. Nevertheless, fibers are the primary factor controlling the properties of fiber-reinforced composite materials. Due to this, there has been a continual effort to use new stiff, strong, lightweight, low-cost, and eco-friendly fibers in composite mate-rials.

2. Materials and methods

The evaluated composite material consists of a matrix made of polyester resin reinforced by six layers of woven glass fabric. In the numerical analysis, the laminate is modelled as symmetric, with 6 layers of thickness 0.5 mm, oriented according to the stacking sequence. Finally, a total thickness of 3 mm is obtained. The model contains the target of 250mm x 25 mm x 3 mm deformable laminated plate and is modelled using Abaqus/CAE. The laminate is stacked in [(0/90)3] S, [(30/-60)3] S and [(45/-45)3] S sequence. The model contains a rectangular thin laminated plate.

2.1. Elastic properties of orthotropic lamina:

The cantilever plate size was 250 mm x 25 mm x 3 mm. The boundary condition of the clamping area is U1 = U2 = U3 = UR1 = UR2 = UR3 = 0. In this simulation, the first three output of natural frequency and mode shape were investigated. In this stage, number of eigenvalues requested or maximum frequency of interest need to define. In the case of fixed-free boundary condition.

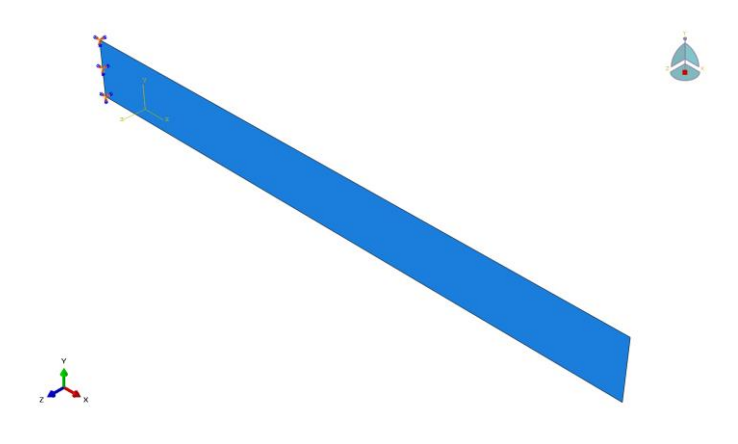


Fig. 1. Boundary Condition

2.2. Experimental program

In the present study, the laminated composite specimens were fabricated by using woven glass fiber and polyester resin as matrix carrying a weight fraction proportion of 50:50. For fabrication, the glass fibers are scissored into definite shapes and sizes as per requirement. The matrix (polyester and hardener) was prepared by using 10% hardener and polyester resin by weight. The woven fiber is arranged in a prescribed sequence on an open mold hand lay-up method used for the fabrication of plies. The mold is placed on a thin aluminum releasing sheet with an application of honey wax 250 as a releasing agent. Polyester resin matrix is deliberately applied to the mold before placing the woven glass fibers to get a polished outer surface and to shield the fibers from environmental exposure. The fabricated sheets are cured manually by putting a heavy load on them for 72 h at room temperature. Utilizing a ruler, the geometric dimension of the beam found as 250 mm in length and 25 mm in width.



Fig. 2. Sample

2.2.1. Free vibration test

Vibration testing can be used as a non-distractive test for structural analysis. The following apparatus are used for free-vibration testing. The DAQ USB NI-6009, an accelerometer ACC-103, lab view 2018 software, test sample. The composite plate test specimens appropriately fitted to the pre-assembled frame which has arrangements for various end conditions. The total setup of the DAQ USB NI-6009, an accelerometer ACC-103, a test sample, and associated cables are shown in Fig 3 Lab view 2018 software is used for vibration measurement. An acceptable coherence is observed for frequency response function (FRF) spectrums.



Fig. 3. Free vibration test

2.3. Numerical results

In this study, preliminary data from manufacturers' manuals about E-glass fiber and polyester are taken. By using the aforementioned equations, these values were evaluated and presented in the table:

Table 1. Glass fiber and polyester matrix properties

Param	eters	Value	
1.	Youngs modulus of glass fiber	70 GPa	
2.	Poison's ratio of glass fiber	0.37	
3.	Glass fiber density	2.5 g/cm ³	
4.	Tensile strength of glass fiber	1.75 GPa	
5.	Shear modulus of glass fiber	30 GPa	
6.	Youngs modulus of polyester	3.5 GPa	
7.	Poison's ratio of polyester	0.25	
8.	Polyester density	1.161 g/cm ³	
9.	Shear modulus of polyester	1.1 GPa	

2.4. Mathematical formulation

The basic configuration of the problem considered here is a woven fiber carbon fiber composite laminated plate of sides as shown in the Figure 1. The lamination se-quence is also shown in Figure 2.

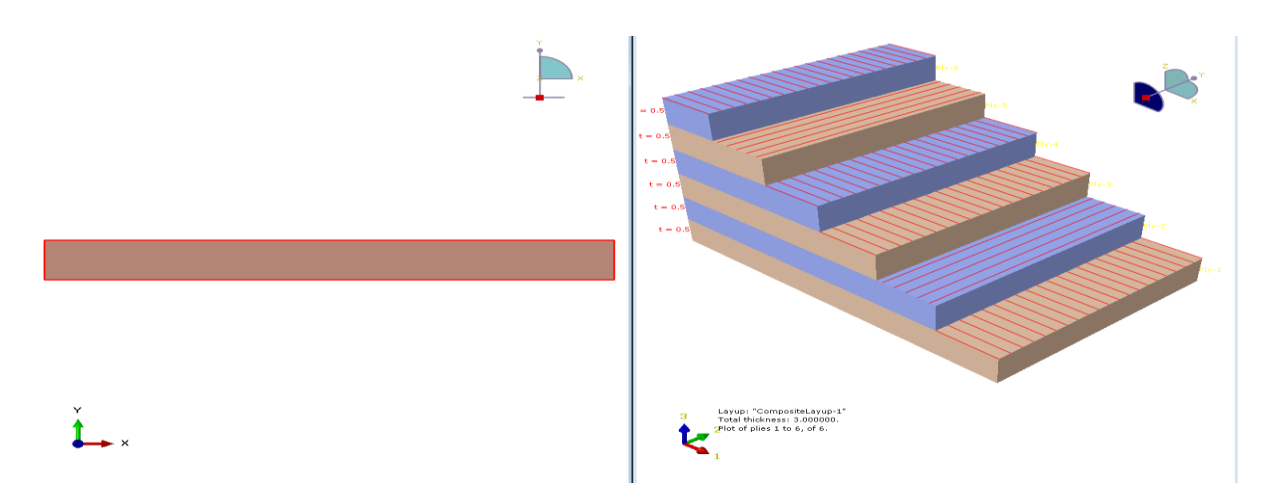


Fig. 4. A. Laminated Composite Plate under in-plane harmonic Loading. B. Lamination sequence.

Based on first-order shear deformation theory, the governing equations for the structural behaviour of the laminated plates are derived. Also, based on the principle of minimum potential energy and Lagrange's equation the element elastic stiffness, geometric stiffness, and mass matrices are derived. The analysis is summarized as follows.

2.4.1. Governing Differential Equation

By taking a differential element of the plate the equation of motion is obtained. Based on first-order shear deformation theory the governing differential equations for vibration of general laminated composite plates derived. To solve the free vibration equation subject to the initial condition, displacement at time t is equal to 0, and velocity at time t equal to 0.

$$m\ddot{u} + ku = 0 \tag{1}$$

In the real world, constant vibration does not happen because you must have vibration systems and it has slowly decay and they slowly come back. How to model this kind that means how to model the energy loss called damping. Energy loss is called damping.

Structural damping:

$$p(t) - ku - c\dot{u} = m\ddot{u} \tag{2}$$

 $m\ddot{u} + c\dot{u} + ku = p(t)$ for forced vibration

Now, this is a fundamental problem that you have in structural dynamics.

Free vibration of a damped structure:

$$m\ddot{u} + c\dot{u} + ku = 0 \tag{3}$$

For the case of dynamic simulation, we use Abaqus/Explicit.

We form the 1. Mass matrix- mü

- 2. Damping matrix- cù
- 3. Stiffness matrix- ku

2.4.2. Finite Element Formulation

Numerical techniques, such as finite element methods, are preferable for issues involving complicated geometry, materials, and boundary conditions because analytical techniques are difficult to adapt. Thus, a finite element formulation is devised for the structural analysis of woven fiber composite plates based on first-order shear deformation theory. In the current analysis, an eight-nodded iso-parametric element has five degrees of freedom (u, v, w, x, and y) per node. Figure 4 depicts the Composite Plate Model, which is a length 'l' and width "d" deformable laminated plate made up of 'n' thin homogeneous orthotropic layers with random orientation and a total thickness of "h". The x-y axes denoted by axes 1–2 is referred to as the reference axes and the primary material axes. The x-axis represents the fiber orientation, while the angle 'θ' is measured counterclockwise. Assumes that the mid-plane normal is not normal even after deformation for the displacement field and remains straight before and after deformation, so that:

The governing equation is:

$$u(x,y,z) = u^{0}(x,y) + z\theta_{x}(x,y) v(x,y,z) = v^{0}(x,y) + z\theta_{y}(x,y) w(x,y,z) = w^{0}(x,y)$$
(4)

Where θ_x , θ_y are the rotations of the cross section normal to the y and x axis and u, v, w are displacements in the x, y, z directions respectively for any point, u_0 , v_0 , w_0 are those at the middle plane of the plate.

2.4.3. Elastic stiffness matrix

The element matrices in natural coordinate system are derived as

$$[k]_{c} = \int_{-1}^{+1} \int_{-1}^{+1} [B]^{T}[D][B]|J|d \,\xi d\eta \tag{5}$$

Where [B] is called the strain displacement matrix

2.4.4. Element mass matrix

$$[M]_e = \int_{-1}^{+1} \int_{-1}^{+1} [N]^T [P][N] |J| d\xi d\eta$$
 (6)

Where the shape function matrix

$$[[N]] = \sum_{i=1}^{8} \begin{bmatrix} N_i & 0 & 0 & 0 & 0 \\ 0 & N_i & 0 & 0 & 0 \\ 0 & 0 & N_i & 0 & 0 \\ 0 & 0 & 0 & N_i & 0 \\ 0 & 0 & 0 & 0 & N_i \end{bmatrix}$$

$$(7)$$

$$[P_1] = \begin{bmatrix} P_1 & 0 & 0 & 0 & 0 \\ 0 & P_1 & 0 & 0 & 0 \\ 0 & 0 & P_1 & 0 & 0 \\ 0 & 0 & 0 & I & 0 \\ 0 & 0 & 0 & 0 & I \end{bmatrix}$$
(8)

In which,

$$P_1 = \sum_{k=1}^n \int_{ek-1}^{ek} \rho dz \text{ and } I = \sum_{k=1}^n \int_{ek-1}^{ek} z^2 \rho dz$$
 (9)

The element load vector due to external transverse static load 'p' per unit area is given by

$$[P]_e = \int_{-1}^{+1} \int_{-1}^{+1} [N_i] \begin{bmatrix} P \\ 0 \\ 0 \end{bmatrix} [J] \, d\xi \, d\eta \tag{10}$$

2.4.5. Elastic properties of composites

Longitudinal tensile modulus along X direction (E11)

$$E_{11} = Eg_f Vg_f + E_m V_m \tag{11}$$

The transverse tensile modulus along Y direction (E22 = E33) is:

$$E22 = (E_f * E_m) / (E_f V_m + E_m V_f)$$
 (12)

Poisson's ratio along XY direction (v12 = v13):

$$\upsilon_{12} = V_f \upsilon_f + V_m \upsilon_m \tag{13}$$

And minor Poisson's ratio:

$$\upsilon_{21} = \frac{E_{11}}{E_{22}} * \upsilon_{12} \tag{14}$$

Shear modulus along XY direction (G12 = G13):

$$G_{12} = (G_f V_m + G_m V_f)$$
 (15)

Shear modulus along YZ direction:

$$G_{23} = \frac{E_{22}}{2(1+v_{23})} \tag{16}$$

ROM

Volume fraction:

$$V, V_c = V_f - V_m \tag{17}$$

Density of composite

$$\rho_{c} = \rho_{gf}. V_{gf} + \rho_{m}.V_{gf}$$

$$\tag{18}$$

Calculated result

$$E_{11} = Eg_f Vg_f + E_m V_m$$

$$E_{11} = 36.75 \text{ GPa}$$

$$E33 = (E_f*E_m)/(E_fV_m + E_mV_f)$$

$$= (70*3.5)/(70*0.5+3.5*0.5)$$

$$E22 = 6.67 \text{ GPa}$$

$$\upsilon_{12}\!\!=\!\!V_f\upsilon_f\!+\!\!V_m\upsilon_m$$

$$\upsilon_{12} = 0.5 * 0.37 + 0.5 * 0.25$$

$$v_{12} = 0.31$$

$$G_{23} = \frac{E_{22}}{2(1+v_{23})}$$

$$v_{23} = \frac{E_{22}}{E_{11}} * v_{12}$$

$$=(6.67/36.75)(0.31)$$

= 0.05626

$$G_{23} = \frac{E_{22}}{2(1+v_{23})}$$

= 3.157 GPa

$$G_{12} = (G_{\rm f} V_{\rm m} {+} G_{\rm m} V_{\rm f})$$

$$=(30*0.5+1.1*05)$$

$$= 15 + 0.55$$

15.55 GPa

$$G_{12} = G_{13}$$

$$G_{13} = 15.55 \text{ GPa}$$

Table 2. Calculated elastic properties of glass-polyester composite material.

S. No.	Parameter	Value
1	E11	36.75 GPa
2	E ₂₂	36.75 GPa
3	E ₃₃	6.67 GPa
4	γ12	0.31

5	G ₁₂	15.55 GPa
6	G ₁₃	3.157 GPa
7	G_{23}	3.157 GPa
8	Density	1830.5 Kg/m ³

3. Results and Discussions

From the vibration test results, the frequency response curves were plotted as shown in Fig. 8-10. The first and second mode natural frequency values are given in Table 3 and 4. It is observed that the first mode natural frequency is dominant for all samples. The natural frequency decreased while the maximum amplitude increased with increasing fiber angle. This is explained by the alignment of fibers in the lamina which contributes to the stiffness of the specimens. In addition, while the fiber angle in-creases from 0° to 45°, the stiffness of the specimen along the longitudinal direction decreases. However, the damping ratio increases while the fiber angle increases from 00 to 450. This may be attributed to the reduction of vibration energy dissipation along the longitudinal direction.

3.1 Simulation Result of Free Vibration of GFRP Materials

The effect of glass fiber, on the first three modal frequencies, was determined by using ABAQUS 2017 software. The natural frequencies of the GFRP materials have been plotted in Figure 5 and 6. The three mode shapes and the corresponding natural frequencies of GFRP in fixed-free end conditions were simulated. It is observed that the stiffness of the composite material increases with the increase in the angle 0-45 of glass fiber. So that the corresponding natural frequencies were decreased.

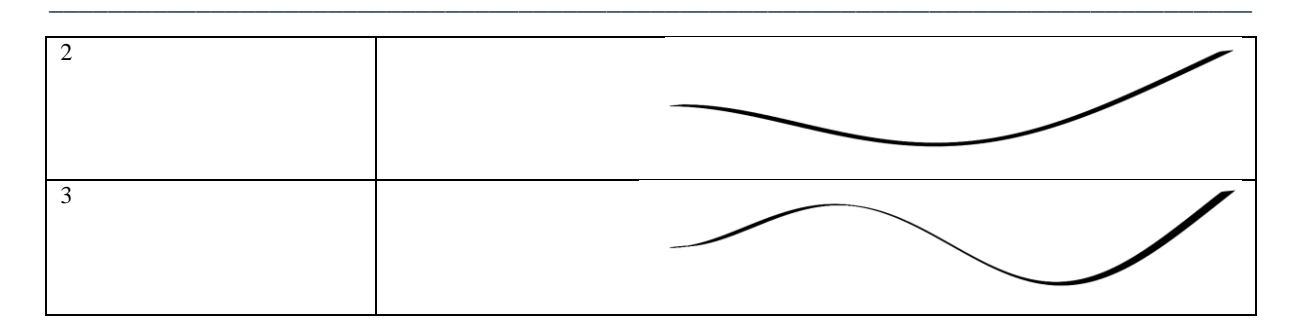
Generally, in this study, the FEA of a cantilever composite material was done in ABAQUS 2017. The mode shapes of the first three modes of free vibration were plot-ted and a comparison of mode shapes of the normal plate was done. It is observed that the natural frequencies of all three transverse modes of vibrations decrease with an increase in the angle from 0 to 45. The frequency of the third mode shape has the highest frequency in mode shapes.

Specimens	Mode 1 (Hz)	Mode 2 (Hz)	Mode 3 (Hz)
0/90	29.581	185.14	517.43
30/-60	28.644	179.27	500.96
45/-45	26.283	164.54	460.01

Table 3. Results of natural frequencies for glass-polyester composite from FEM.

Table 4. FEA of 0/90 for fixed-free boundary condition bending mode shapes.

Mode	FEM
1	



It is observed that first mode natural frequency is clearly dominant for all samples. The natural frequency decreased while maximum amplitude increased with increasing fiber angle. This is explained by the alignment of fibers in the lamina which con-tributes to the stiffness of the specimens. In addition, while the fiber angle increases from 0° to 45°, stiffness of the specimen along the longitudinal direction decreases.

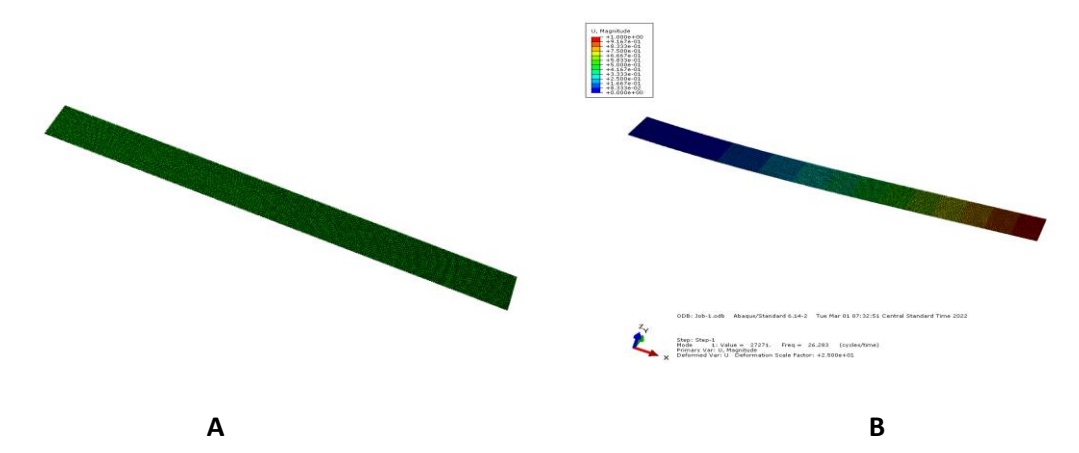


Fig. 5. Fig. show (a) Meshing of element; (b) mode 1 post-processing stage.

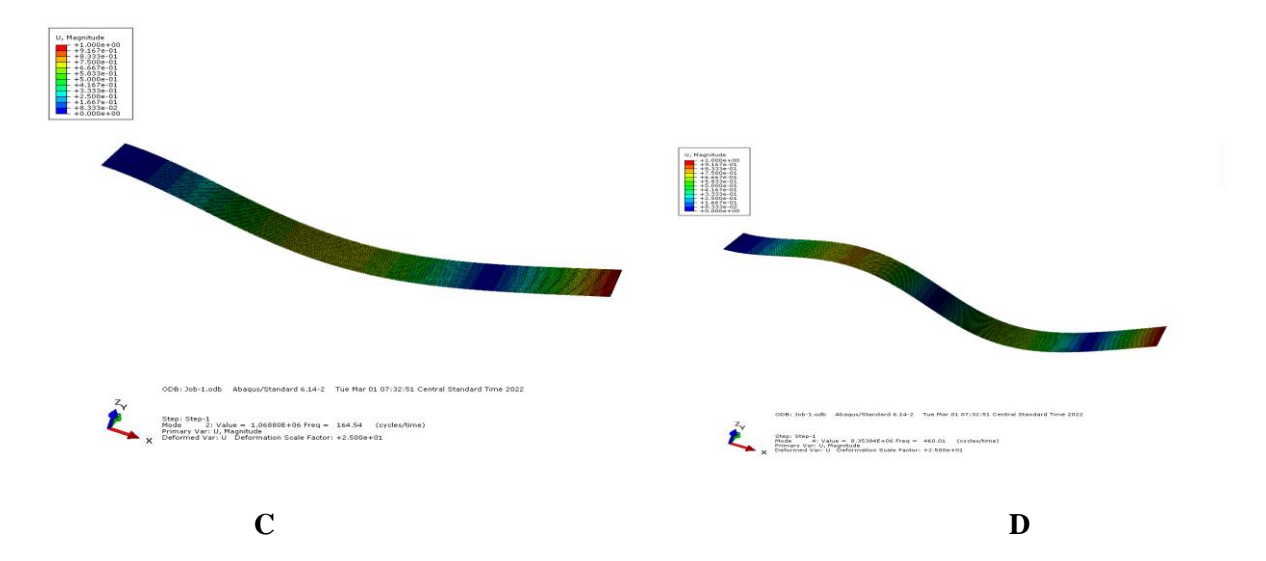


Fig. 6. show (c) mode 2 post-processing stage.; (d) mode 3 post-processing stage.

This is attributed to the reduced dissipation of vibrational energy along the longitudinal direction. The increase of effective damping could be causing a reduction of energy dissipated and responses by means of amplitudes. It can

be concluded that the increase of fiber angle of glass-polyester composite laminates from 0° to 45° de-creased the natural frequency while increasing the damping ratios.

3.2. Experimental Results of Free Vibration of GFRP Materials

Through the experimental setup, that is, an accelerometer ACC-103 attached at the end of the specimen by wax and the DAQ USB NI-6009 was connected to the computer with the help of lab view 2018 software, then the natural frequencies of the cantilever GFRP materials were recorded on MATLAB by the use of block diagram of lab view software.

3.2.1. Damping Ratio and Natural Frequencies of GFRP Materials

In the free vibration experimental investigation, the amplitude and frequency of oscillations were affected by the damping properties of the materials. Figures 8-10 show the first mode of damping responses for the cantilever beam of GFRP. The damping of composite material trends was observed with the increase in the content of angle from 0 to 45 glass fiber for the former damping increased. Through the same experimental setup and DAQ analysis, the natural frequencies for the cantilever beam of GFRP are plotted on the linear scales shown in Figures 8-10 the results are plotted.

3.2.2. **Damping Ratio**

In order to measure damping responses, half power band-width method was used for first natural frequency mode of the specimen. The damping ratio was measured ac-cording to the half band-width method as shown in Fig. 7, according to Eq. (19)

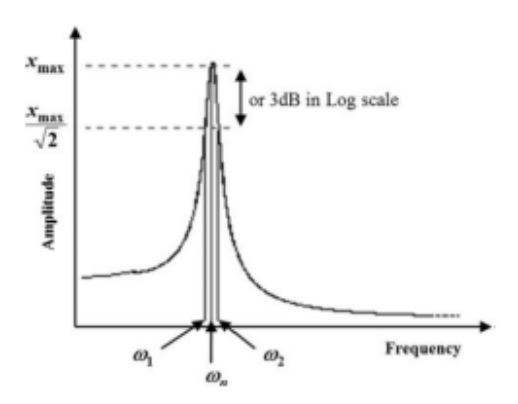
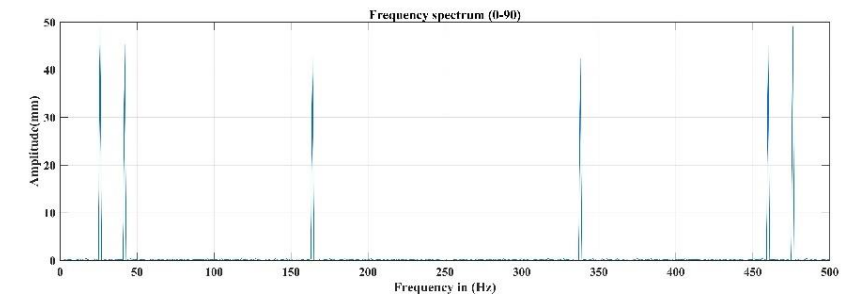


Fig. 7. Half power band-width method.

$$\xi = \frac{\omega_1 - \omega_2}{2\omega_n} \tag{19}$$

Where $\omega 1$, $\omega 2$ are the bandwidth, ωn is the natural frequency of first mode, and ξ is the damping ratio.



Vol. 45 No. 2 (2024)

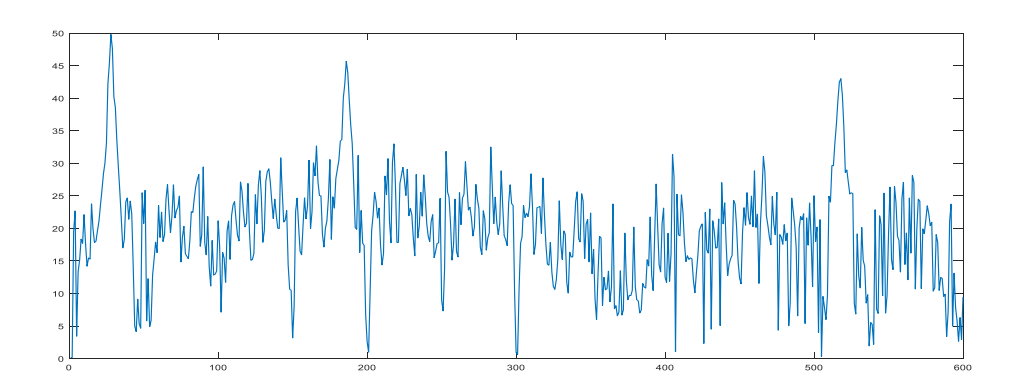


Fig. 8. Frequency Response Function (FRF) of GFRP (0/90).

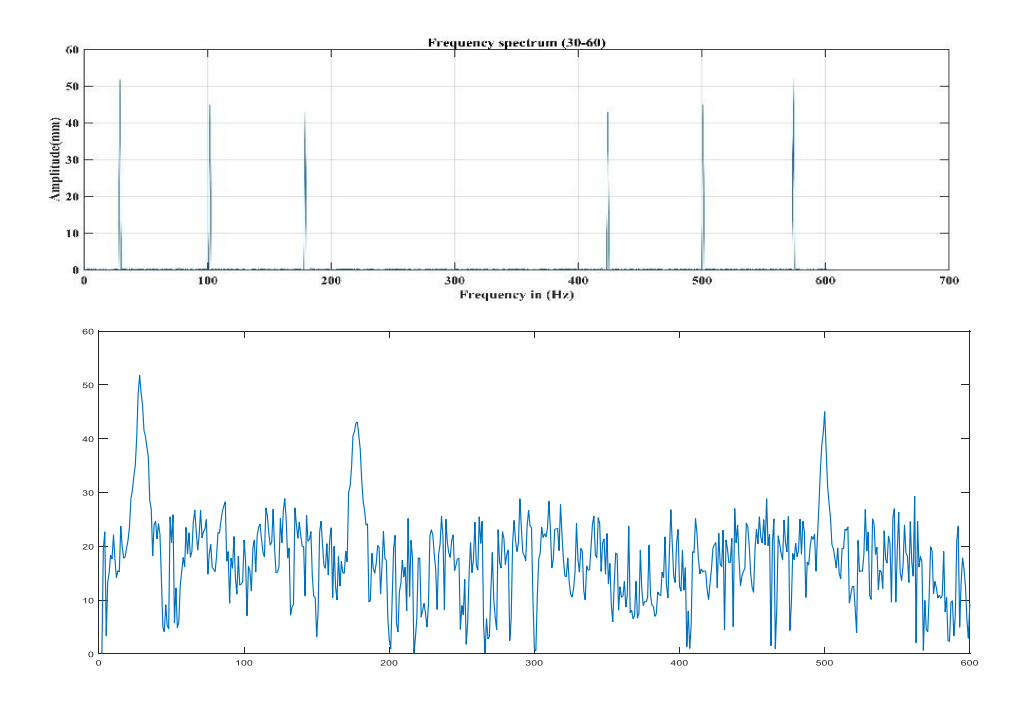
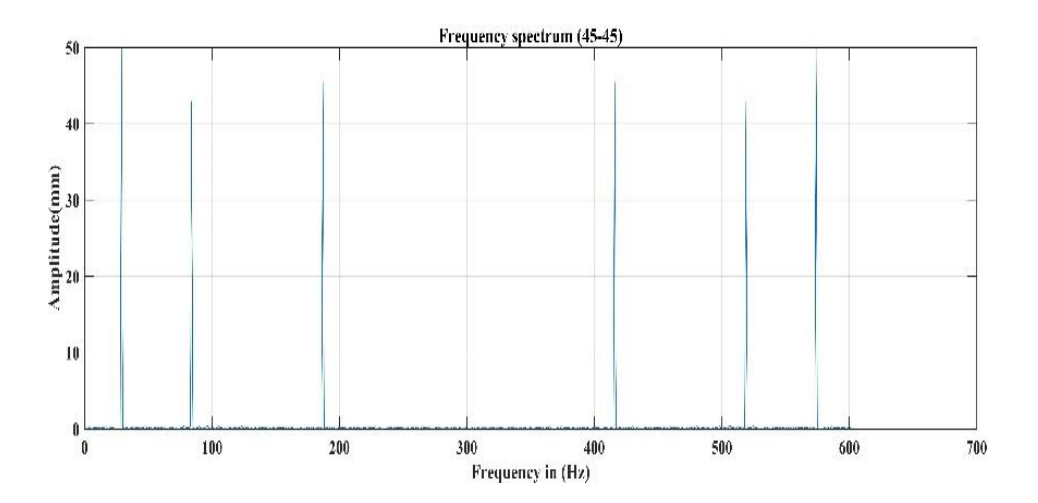


Fig. 9. Frequency Response Function (FRF) of GFRP (30/60).



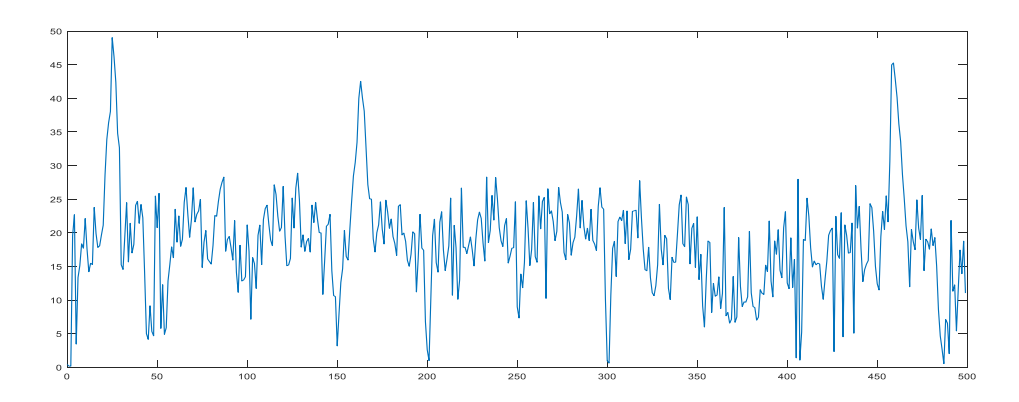


Fig. 10. Frequency Response Function (FRF) of GFRP (45/-45).

Table 5: The experimental value of natural frequency and damping ratio of GFRP materials.

Composite plate	Mode	Natural frequency (Hz)	Damping ratio (ζ)
	1	28	0.11607
0/90	2	186	0.02284
	3	518	0.00481
	1	28	0.15535
30/60	2	178	0.023
	3	500	0.0055
	1	25	0.18
45/-45	2	163	0.02595
	3	459	0.006209

Table 5 shows the natural frequencies and damping ratios recorded from GFRP materials by experimental methods. The fundamental mode shapes of GFRP materials provide insight into the selection of materials for suitable structural applications. In this study, the natural frequencies of the GFRP materials are inversely proportional to the damping ratios. In addition, the magnitude of the natural frequency and damping ratio of the GFRP were significantly influenced by the fiber angle orientation composite materials. The maximum natural frequency was found from the 00/900 angle orientation as indicated by the frequency response function (FRF) curve shown in Figures 8-10. And also, the maximum damping ratio was found from 450/-450.

3.2.3. The Comparisons Between Numerical and Experimental Results of Natural Frequency

Table 6: The result comparison of the first natural frequencies recorded from GFRP materials by numerical and experimental methods.

Composite plate	mode	Numerical	Experimental	% Error
	1	29.581	28	5.34
0/90	2	185.14	186	0.464
	3	517.43	518	0.1106
	1	28.644	28	2.248
30/60	2	179.27	178	0.708
	3	500.96	500	0.192

	1	26.283	25	4.88
45/-45	2	164.54	163	0.936
	3	460.01	459	0.219

3.2.4. The principle of deriving Yong's modulus from vibration measurements

The dynamic method involved to calculate Young's modulus base on the univocal relationship between it and the dimensions, weight and natural frequencies of the beam for a given support configuration. Knowing the end conditions, we can express the mathematical relation between Young's modulus E and the beam dimensions L, B respectively H, weight m and natural frequencies fi, as:

$$E = \frac{mL^3}{I} \left(\frac{2\pi f_i}{\alpha_i^2}\right)^2 \tag{20}$$

where I is the moment of inertia of plain area, derived as $I = (B \cdot H3)/12$, and αi are coefficients related to the beam's support condition and the mode numbers. Table 1 presents the first six coefficients derived for the beam with fixed-free end conditions (cantilever beam).

Table 7: Dimensionless coefficients for calculating the frequencies of the cantilever beam.

Mode No.	1	2	3
α _i [-]	1.87510	4.69409	7.85476

Table 8: Results of Young's modulus.

	Young's modulus E [GPa].			
Specimens	Mode 1	Mode 2	Mode 3	
0/90	31.39	32.879	32.529	
30/-60	29.2633	30.1119	30.3049	
45/-45	23.3285	25.25077	25.5387	

The natural frequency of a system increases with increases in the stiffness of the system. It also shown in table 8.

4. Conclusions

Experiments were conducted on glass fiber- reinforced polymer (GFRP). Laminate composite specimens with varying fiber orientation to evaluate the residual elastic behaviour. Hence software is used to evaluate the vibration modulus of any orientation. It is observed from the result that glass polyester with 00/900 fiber orientation Yields high residual elastic when compare to other degrees of orientations for the same load, size & shape in addition.

Damping and vibration characteristics of glass-polyester composite laminates were determined and the effect of fiber orientation was evaluated. Using the logarithmic decrement method, the damping properties were obtained from vibration response envelope curves. The main conclusions of this study can be summarized as follows:

- Damping and vibration characteristics of the composite samples are affect-ed by the fiber orientation of glass-polyester,
- \triangleright The increase in the angle of fiber orientation from 0°- 45° resulted in a de-crease in natural frequency,
- The laminates having higher fiber orientation angles had higher damping ratios,

Finally, the results suggest that it can be possible to obtain the desired damping and vibration capability by altering the orientation angles of GFRP.

Refrences

[1] Schwaar, M., T. Gmur, and J. Frieden, Modal numerical-experimental identification method for characterizing the elastic and damping properties in sandwich structures with a relatively stiff core. Composite Structures, vol. 94, pp. 2227-2236, 2012.

- [2] Xu, Y.F. and W.D. Zhu, Operational modal analysis of a rectangular plate using noncontact excitation and measurement. Journal of Sound and Vibration, vol. 332, pp. 4927-4939, 2013.
- [3] Barkanov, E., et al., An effectiveness improvement of the inverse technique based on vibration tests. Computers & Structures, vol. 146, pp. 152-162, 2015.
- [4] Sato, J., I.M. Hutchings, and J. Woodhouse, Determination of the dynamic elastic properties of paper and paperboard from the low-frequency vibration modes of rectangular plates. Appita Journal, vol. 61, pp. 291-296, 2008.
- [5] Ragauskas, P. and R. Belevičius, Identification of material properties of composite materials. Aviation, vol. 13, pp. 109-115, 2009.
- [6] Zubaidah Ismail, H.K., and Wen L. Li, Identifying material properties of composite materials from vibration data. World Journal of Engineering, vol. pp. 2011.
- [7] N. Yokoyama, M. Donadon, and S. J. C. S. De Almeida, "A numerical study on the impact resistance of composite shells using an energy-based failure model," vol. 93, no. 1, pp. 142-152, 2010.
- [8] J. Gieske and R. J. E. M. Allred, "Elastic constants of B-A1 composites by ultrasonic velocity measurements," vol. 14, no. 4, pp. 158-165, 1974.
- [9] S. Rokhlin and W. Wang, "Ultrasonic evaluation of in-plane and out-of-plane elastic properties of composite materials," in Review of Progress in Quantitative Nondestructive Evaluation: Springer, 1989, pp. 1489-1496.
- [10] Montalvão, D.; Maia, N.M.M.; Ribeiro, A.M.R. A review of vibration-based structural health monitoring with special emphasis on composite materials. Shock Vib. Dig. 2006, 38, 295–324.
- [11] S. S. Rahimian Koloor, A. Karimzadeh, N. Yidris, M. Petrů, M. R. Ayatollahi, and M. N. J. P. Tamin, "An energy-based concept for yielding of multidirectional FRP composite structures using a mesoscale lamina damage model," vol. 12, no. 1, p. 157, 2020.
- [12] H.-J. Steenhuis and E. J. de Bruijn, "Building theories from case study research: the progressive case study," in OM in the New World Uncertainties. Proceedings (CD-ROM) of the 17th Annual Conference of POMS, 28 April-1 May 2006, Boston, USA, 2006, pp. 546-558: Production and Operations Management Society (POMS).
- [13] Cawley, P.; Adams, R.D. The location of defects in structures from measurements of natural frequencies. J. Strain Anal. 1979, 14, 49–57.
- [14] D. Montalvao, N. M. M. Maia, A. M. R. J. S. Ribeiro, and v. digest, "A review of vibration-based structural health monitoring with special emphasis on composite materials," vol. 38, no. 4, pp. 295-324, 2006.
- [15] J. M. Lifshitz and A. J. J. o. C. M. Rotem, "Determination of reinforcement unbonding of composites by a vibration technique," vol. 3, no. 3, pp. 412-423, 1969.
- [16] K. E. Fällström and M. J. P. C. Jonsson, "A nondestructive method to determine material properties in anisotropic plates," vol. 12, no. 5, pp. 293-305, 1991.
- [17] Larsson, D. Using modal analysis for estimation of anisotropic material constants. J. Eng. Mech. 1997, 123, 222–229.
- [18] Fällström, K.-E.; Jonsson, M. A nondestructive method to determine material properties in anisotropic plates. Polym. Compos. 1991, 12, 293–305.
- [19] Caldersmith, G.W. Vibrations of orthotropic rectangular plates. Acustica 1984, 56, 144 152.
- [20] C. J. A. S. Boursier Niutta, "Enhancement of a new methodology based on the impulse excitation technique for the nondestructive determination of local material properties in composite laminates," vol. 11, no. 1, p. 101, 2020.
- [21] S. Abrate, Impact on composite structures. Cambridge university press, 1998.
- [22] Borza, D.N., Vibration-based identification of isotropic material properties by quasibinary electronic holography and finite element modelling. Inverse Problems in Science and Engineering, vol. 12, pp. 45-57, 2004.